CrystEngComm

COMMUNICATION

View Article Online
View Journal | View Issue

Cite this: *CrystEngComm*, 2017, **19**, 3557

Received 4th April 2017,
Accepted 1st June 2017

DOI: 10.1039/c7ce00642j

rsc.li/crystengcomm

A crab claw shaped molecular receptor for selective recognition of picric acid: supramolecular self-assembly mediated aggregation induced emission and color change†

Jayaraman Pitchaimani,‡[a] Anu Kundu,‡[b] Subramanian Karthikeyan,[c] Savarimuthu Philip Anthony, *[b] Dohyun Moon*[d] and Vedichi Madhu*[a]

2,6-Pyridine bis(iminoantipyrine) (PyBAP), a crab claw shaped open neutral molecular receptor with multiple non-covalent sites, showed selective recognition of picric acid (PA) through supramolecular interactions that lead to an intermolecular charge transfer induced naked-eye detectable color change both in solution as well as in the solid state and rare turn-on solid state fluorescence. The selective host–guest formation of PyBAP–PA has been confirmed using ^{1}H-NMR, single crystal structural analysis and computational studies.

Molecular recognition and supramolecular self-assembly, two very important core concepts, have received significant attention from researchers over the years for gaining insight and control over bio-molecular self-assembly and functions.[1] Advancement in molecular recognition roused interest in biological processes, such as enzymatic activity, allosteric regulation, molecular transport, genetic information, protein assembly, sensing and separation.[2] In particular, the developing neutral molecular recognition received special focus because of its relevance to biological and environmental sciences.[3] Supramolecular interactions including hydrogen bonding, metal–ligand coordination, electrostatic, van der Waals and π···π-stacking interactions as well as the shape of the molecules exerted strong control over molecular recognition.[4] Tailor-made molecular receptors with multiple non-covalent interaction sites are proposed as good model systems for understanding the complexity of molecular recognition and demonstrating the biological "lock and key" fitting mechanism between enzymes and their substrates.[4,5] Hence several synthetic molecular receptors mostly with a macrocyclic scaffold structure, such as crown ethers,[6] calixarenes,[7] cucurbiturils,[8] cyclodextrins,[9] polyaza macrocycles,[10] *etc.*, have been synthesized and their molecular recognition towards metal cations, anions and chiral molecules explored.[11] Polyaza macrocycle based receptors showed selective recognition of sulphate anions over other ions with high association constants and remarkable fluorescence enhancement.[12] Supramolecular self-assembly of cucurbituril (CB[*n*]) based artificial receptors has been exploited for molecular recognition of neutral molecules as well as ions.[13] Picolyl amide functionalized calixarene and coumarine–Se_2N chelating conjugates exhibited selective recognition of Ag^+ ions *via* turn-on fluorescence.[14] A bowl shaped organic host with bispyridine ligands showed selective recognition of aromatic carbonyls.[15] Selective recognition of nitroaromatic explosives (NAEs) using molecular receptors has become an important field of research in recent years owing to its applications in security and environmental pollution.[16] Particularly, picric acid (PA), an environmental pollutant, that has a superior explosive power to TNT and wide usage, demands more attention.[17] Bimetallic Schiff base complexes with an ester functionality at the periphery structure showed selective turn-off fluorescence for PA.[18] An aggregation induced emissive tetraphenylethylene macrocycle also showed turn-off fluorescence for PA.[19] There are a few other fluorescent molecular sensors including triphenylamine based small molecules that have also been reported for PA sensing.[20] However, small molecular receptors with non-cyclic structures that exhibit selective turn-on fluorescence especially in the solid state and naked-eye detectable color changes for PA are rarely reported,[21] although they

[a] *Department of Chemistry, School of Science & Humanities, Karunya University, Coimbatore-641114, Tamil Nadu, India. E-mail: madhu@karunya.edu; Tel: +91 422 261 4483*

[b] *School of Chemical & Biotechnology, SASTRA University Thanjavur-613401, Tamil Nadu, India. E-mail: philip@biotech.sastra.edu*

[c] *Department of Chemistry, Kalasalingam University, Krishnan Kovil-626126, India*

[d] *Beamline Department, Pohang Accelerator Laboratory, 80 Jigokro-127 beongil Namgu, Pohang, Gyeongbuk, Korea. E-mail: dmoon@postech.ac.kr*

† Electronic supplementary information (ESI) available: Synthesis, NMR data, absorption spectra, crystallographic table of PyBAP and PyBAP–PA, crystal structures, PXRD pattern and excitation spectra. CCDC 1534730 and 1534731. For ESI and crystallographic data in CIF or other electronic format see DOI: 10.1039/c7ce00642j

‡ These authors equally contributed.

require a simple visual detection method in classical chemical analysis. The non-cyclic receptors with conformationally flexible structures might provide adaptive cavities in recognizing guest species.[22] In this context, redox active bis(imino)-pyridine based receptors could be interesting because of their ability to exhibit various resonance forms[23] that could be utilized for fabricating electrochemical sensors.[24] Herein, we report the selective recognition of PA by PyBAP, a crab claw shaped open molecular receptor with multiple non-covalent sites, both in the solid as well as solution state (Scheme 1). PyBAP in CH_2Cl_2 selectively produced an orange-red color from colorless upon adding PA. The absorption spectrum revealed a new intermolecular charge transfer (CT) peak at 500 nm. The solid mixture of PyBAP–PA also showed an orange-red color with CT absorption at 545 nm. Structural analysis confirmed the incorporation of PA in between PyBAP claws *via* supramolecular interactions. Surprisingly, the hydroxyl group of PA did not show deprotonation in the solid state. The inclusion of PA rigidified the molecular structure of PyBAP by extended supramolecular interactions that lead to rare turn-on aggregation induced emission (620 nm). The selective molecular recognition by PyBAP was further supported by ^{1}H-NMR and computational studies.

PyBAP was synthesized by a simple condensation reaction between 2,6-pyridinedicarboxaldehyde and 4-aminoantipyrine in refluxing ethanol (Scheme S1†). PyBAP crystallized in the monoclinic space group $P2_1/n$ and displayed a crab claw shaped molecular structure (Fig. S3 and Table S1†). The multiple non-covalent interaction sites and open claw shaped molecular structure could be of potential interest for molecular recognition. Interestingly, addition of PA into a CH_2Cl_2 solution of PyBAP selectively produced an orange-red color (Fig. 1). PyBAP showed absorption at 356 nm whereas PA showed a broad absorption peak at 369 nm with a small hump at 427 nm (Fig. S4†). However, addition of PA into PyBAP showed a new CT peak at 500 nm. Addition of other nitroaromatic compounds (NACs) including closely competitive 2,4-dinitrophenol did not show a significant color or absorption change. The appearance of a clear new CT peak while adding PA into PyBAP in the presence of other NACs confirmed the good selectivity (Fig. S5†). In most of the previously reported receptor, dinitrophenol interfered strongly with the selectivity of PA.[25] Similar to the solution, grinding of PyBAP solids with PA has also produced a visible color change from colourless to orange-red that showed CT absorption at 545 nm (Scheme 1 and Fig. S6†). But grinding of other nitroaromatic compounds with PyBAP did not produce a significant color change except 4-nitrophenol that produced a light orange color (Fig. S7†). However, the subsequent mixing of PA leads to a clear reddish orange color. These results further substantiated the selective recognition of PA by the PyBAP molecular receptor over other NACs including closely resembling dinitrophenol.

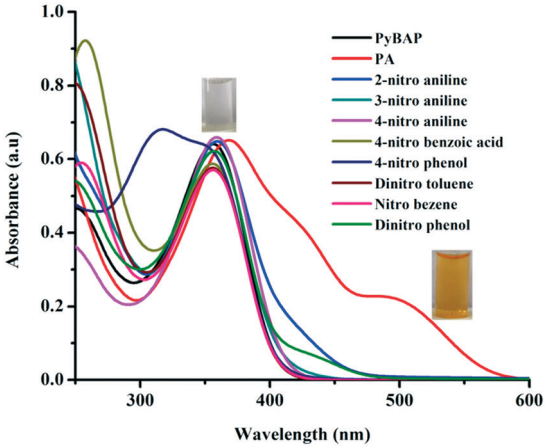

Fig. 1 Absorption spectra of PyBAP (10^{-3} M) with different nitroaromatic compounds (10^{-3} M). Digital image shows the selective color change of PyBAP solution for PA.

To gain insight into the molecular recognition by PyBAP, single crystals of host–guest PyBAP–PA were grown from CH_2Cl_2 by mixing at a 1 : 1 molar ratio. Slow diffusion of diethyl ether vapor into CH_2Cl_2 produced orange-red crystals. Structural analysis revealed the formation of a 1 : 1 PyBAP–PA host–guest structure in the solid state (Fig. 2a, S8 and Table S2†). The PyBAP molecular receptor displayed different conformations in the crystal lattice of PyBAP and the PyBAP–PA host–guest compound (Fig. 2b). The phenyl groups of antipyrine adopted a nearly coplanar structure in the PyBAP–PA host–guest complex (τ = 79.41 and 75.23 (PyBAP–PA)) whereas a more planar as well as a perfect coplanar conformation was observed in PyBAP (τ = 56.34 and 91.26 (PyBAP, Fig. S9†)). Apart from the conformational change, the antipyrine claws exhibited a slightly more inward twist in the PyBAP–PA crystal lattice compared to pure PyBAP (Fig. 2b). The deprotonated hydroxyl group of PA formed strong intermolecular H-bonding with

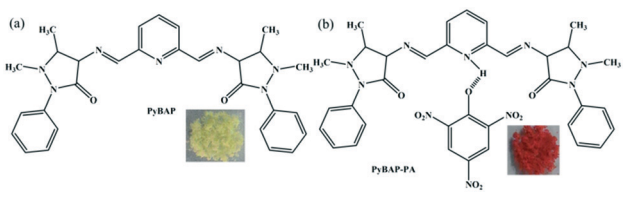

Scheme 1 Molecular structure of (a) the PyBAP receptor and (b) the PyBAP–PA host–guest complex. The inset shows the digital images of PyBAP and PyBAP–PA solids.

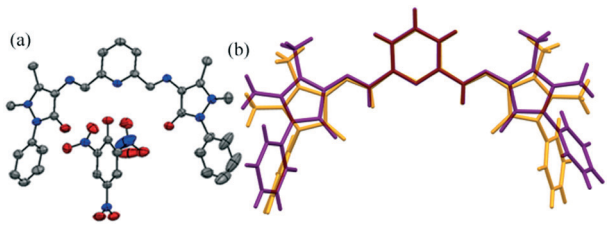

Fig. 2 (a) ORTEP diagram of PyBAP–PA with a 50% probability ellipsoid and H-atoms are omitted for clarity. (b) Different conformations of PyBAP in the crystal lattice of PyBAP and PyBAP–PA.

protonated pyridine nitrogen ($d_{D\cdots A}$ = 2.678(5) Å, Fig. 3a). This strong H-bonding intermolecular interaction draws PA closer to the pyridine unit. The PA molecule in between the antipyrine claws adopted a coplanar conformation with respect to pyridine and a face to face orientation to the two antipyrine phenyl groups that facilitate intermolecular CT (Fig. S9†). The antipyrine phenyl group of PyBAP molecules are interdigitated between PA and another PyBAP antipyrine phenyl group along the *b*-axis (Fig. 3 and S10–11). The strong C–H···O intermolecular interactions ($d_{D\cdots A}$ = 3.081(5) Å) between phenyl hydrogen and antipyrine carbonyl stabilized the interdigitation. Further the interdigitated phenyl group formed π···π interactions with PA (3.434 Å). The receptor, PyBAP and PA assembled into a supramolecular chain like structure through the combination of C–H···O ($d_{D\cdots A}$ range = 3.081(5)–3.709(4) Å and bond angles range = 122.37–147.39°) and π···π interactions between PA and PyBAP in the crystal lattice along the *b*-axis (Fig. 3a). The PA molecules have been trapped in between the channel formed by the interdigitation of the PyBAP phenyl group (Fig. 3b). The nitro group of PA interacts with five different PyBAP molecules *via* C–H···O intermolecular interaction that further connects the network in the crystal lattice (Fig. S12†). It is noted that pure PyBAP did not show any interdigitated or π···π stacking arrangement, rather the weak C–H···O intermolecular interactions produced helical and sheet structures (Fig. S13 and 14). Thus, the incorporation of PA in between the antipyrine claws might be induced by the synergistic interaction of H-bonding between protonated pyridine nitrogen and the deprotonated hydroxyl of PA and π···π interactions between antipyrine phenyl and PA. The perfect matching of the experimental and simulated PXRD patterns of PyBAP–PA confirmed the phase purity of the sample (Fig. S15†).

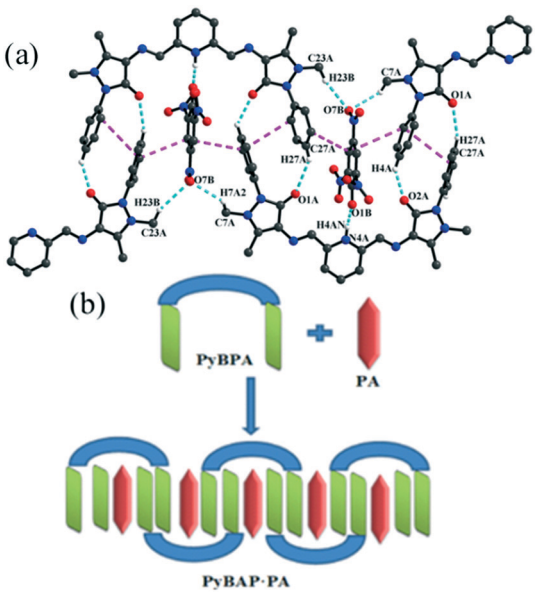

Fig. 3 (a) The supramolecular interactions in the crystal lattice of the PyBAP–PA host–guest compound (hydrogen-bond, cyan line; π–π interaction, purple line). (b) Schematic representation of the supramolecular self-assembly in PyBAP–PA *via* molecular recognition.

The intense color change of PyBAP with PA could be attributed to intermolecular CT between electron rich antipyrine to electron poor PA. The interdigitation of PA between antipyrine phenyl groups *via* extended π···π stacking further supports the CT. The ^{1}H-NMR spectra of PyBAP–PA showed only a small up field shift of the imine proton and a slight down field shift of some of the aromatic protons (Fig. S2†). The intermolecular CT has also been supported by computational studies. The single crystal structures of PyBAP and PyBAP–PA and the optimized structure of pyridine nitrogen protonated PyBAP (PyBAP-H) have been used for the calculation (Fig. S16†). The isodensity surface plot (isodensity contour = 0.02) of the highest occupied molecular orbitals (HOMOs) and the lowest unoccupied molecular orbitals (LUMOs) of PyBAP–PA indicated clear charge transfer from PyBAP to PA (Fig. S17†). The calculated HOMO–LUMO band gap also suggested a strong red shift of absorption for PyBAP–PA (2.12 eV, 584 nm) compared to PyBAP (3.72 eV, 333 nm, Table S3†). PyBAP and PyBAP-H showed an intramolecular charge transfer transition from the antipyrine unit to the pyridine unit.

PyBAP did not show any fluorescence both in the solution as well as solid state. Interestingly, the incorporation of PA in between the PyBAP claws rigidified the PyBAP molecule in the solid state through multiple supramolecular interactions (H-bonding, C-H···O and π···π stacking interactions) that led to orange fluorescence (620 nm) in the solid state (Fig. 4a). The excitation spectra and solid state absorption spectra of PyBAP–PA are similar (Fig. S6 and S18†). However, in solution, PyBAP–PA did not show any fluorescence. Thus the incorporation of PA with PyBAP in the crystals leads to rare turn-on solid state fluorescent host–guest materials that included nitroaromatic compounds. The turn-on fluorescence could be attributed to the restriction of the intramolecular rotation (RIR) of imine *via* molecular aggregation, which is generally called aggregation induced emission (AIE).[26,27] The orange fluorescence of PyBAP–PA could be attributed to the formation of an intermolecular charge transfer complex between PyBAP and PA in the solid state along with RIR. The molecular recognition of PA by PyBAP has also been exploited to demonstrate selective visible color changes on a paper strip (Fig. 4b). PA vapour exposure on a PyBAP solid coated

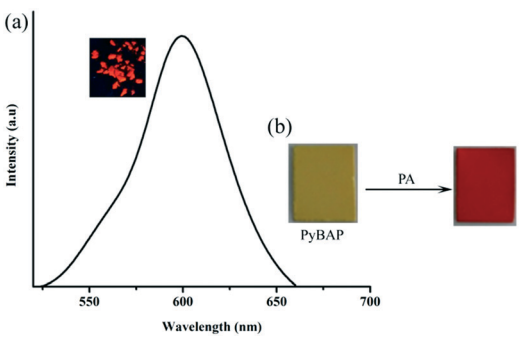

Fig. 4 (a) Fluorescence spectra of PyBAP. (b) Color change of a PyBAP coated paper strip after dipping into an aqueous solution of PA (10^{-2} M).

paper strip showed a clear color change from pale yellow to red. Similarly, the PyBAP paper strip exhibited a selective color change upon dipping into an aqueous solution of PA (10^{-2} M) whereas dipping into other NAC solutions did not show any significant change. The PyBAP paper strips have also been dipped in different concentrations of an aqueous solution of PA (Fig. S19†). The paper strip dipped in 10^{-3} M PA solution showed a clear color change. However, dipping in below 10^{-3} M solution did not show any visible color change. Hence PyBAP can detect up to a 10^{-3} M concentration of PA. Thus crab claw shaped PyBAP recognized PA selectively through multiple supramolecular interactions both in solution as well as the solid state that caused a visibly detectable selective color change. It is noted that most of the reported colorimetric or turn-off/turn-on fluorescence chemosensors experienced significant interference from other NACs particularly from 4-nitrophenol and 2,4-dinitrophenol.[20,21,25] In contrast, synergistic weak intermolecular interaction induced and molecular shape controlled PyBAP sensing of PA did not show any significant interference from other NACs.

Conclusions

In summary, PyBAP, a crab claw shaped open neutral molecular receptor showed selective molecular recognition of PA over other NACs including 2,4-dinitrophenol in solution as well as in the solid state. A colorless CH_2Cl_2 solution of PyBAP turned red-orange upon addition of PA. Similarly grinding as well as host–guest complex formation of PyBAP with PA also produced a red-orange solid. The absorption spectra showed a new charge transfer peak at 500 nm in solution and 545 nm in the solid state. The solid state structural analysis confirmed the formation of a 1 : 1 host–guest complex of PyBAP–PA. The interdigitation and extended $\pi\cdots\pi$ interactions between antipyrine phenyl and PA facilitated the intermolecular charge transfer that led to the intense orange-red color of PyBAP–PA. Interestingly, PyBAP showed rare PA induced turn-on fluorescence in the solid state due to the rigidification of the PyBAP receptor by multiple supramolecular interactions. These results highlight the role of the molecular shape and multiple non-covalent interaction sites in the selective recognition of NACs. The present study suggests that the open crab claw shaped conformationally flexible molecular receptor could be a potential molecule for recognizing electron poor NACs. The tailorable electron donor capacity of antipyrine/pyridine and further inward orientation of the antipyrine unit *via* conformational flexibility along with a H-bonding functionality might facilitate better recognition and faster response to electron poor NACs. Currently, our research work is focused on exploring the role of substituents that would change the donor/acceptor properties of antipyrine/pyridine units in the selective molecular recognition of NACs.

Financial support from the DST, New Delhi, India (Grant scheme no. SB/FT/CS-182/2011 and EMR/2015/00-1891) is acknowledged. VM is grateful to UGC, India for the UGC research award (No. F. 30-11/2015(SA-II).

Notes and references

1 Synthetic Receptors for Polar Lipids, K. J. Clear and B. D. Smith in *Synthetic Receptors for Biomolecules: Design Principles and Applications*, ed. B. D. Smith, Royal Society of Chemistry, Cambridge, UK, 2015.

2 (*a*) P. A. Gale, *Acc. Chem. Res.*, 2011, **44**, 216; (*b*) M. Cacciarini, V. A. Azov, P. Seiler and F. Diederich, *Chem. Commun.*, 2005, 5269; (*c*) M. M. Safont-Sempere, G. Fernandez and F. Wurthner, *Chem. Rev.*, 2011, **111**, 5784; (*d*) E. Persch, O. Dumele and F. Diederich, *Angew. Chem., Int. Ed.*, 2015, **54**, 2.

3 (*a*) J. L. Sessler, P. Gale and W.-S. Cho, *Anion Receptor Chemistry*, Royal Society of Chemistry, Cambridge, UK, 2006; (*b*) Y. Ferrand, M. P. Crump and A. P. Davis, *Science*, 2007, **318**, 619; (*c*) H. L. Liu, Q. Peng, Y.-D. Wu, D. Chen, X. L. Hou, M. Sabat and L. Pu, *Angew. Chem., Int. Ed.*, 2010, **49**, 602; (*d*) D. E. Horner, D. J. Crouse, K. B. Brown and B. Weaver, *Nucl. Sci. Eng.*, 1963, **17**, 234; (*e*) R. Sheng, L. Tang, L. Jiang, L. Hong, Y. Shi, N. Zhou and Y. Hu, *ACS Chem. Neurosci.*, 2016, **7**, 69.

4 (*a*) F. Biedermann and H.-J. Schneider, *Chem. Rev.*, 2016, **116**, 5216; (*b*) A. Kalita, S. Hussain, A. H. Malik, U. Barman, N. Goswami and P. K. Iyer, *ACS Appl. Mater. Interfaces*, 2016, **8**, 25326; (*c*) J.-M. Lehn, *Angew. Chem., Int. Ed. Engl.*, 1990, **29**, 1304; (*d*) X. Ma, A. Urbas and Q. Li, *Langmuir*, 2012, **28**, 16263; (*e*) R. Sun, C. Xue, X. Ma, M. Gao, H. Tian and Q. Li, *J. Am. Chem. Soc.*, 2013, **135**, 5990–5993; (*f*) R. Sun, H. K. Bisoyi, M. Xie and Q. Li, *Dyes Pigm.*, 2016, **132**, 336.

5 E. Fischer, *Chem. Ber.*, 1894, **27**, 2985.

6 (*a*) Y. Han, Z. Meng, Y.-X. Ma and C.-F. Chen, *Acc. Chem. Res.*, 2014, **47**, 2026; (*b*) C. Liu, D. Walter and D. Neuhauser, *J. Am. Chem. Soc.*, 2003, **125**, 13936.

7 (*a*) D. S. Kim and J. L. Sessler, *Chem. Soc. Rev.*, 2015, **44**, 532; (*b*) M. X. Wang, *Acc. Chem. Res.*, 2012, **45**, 182; (*c*) C. H. Lee, H. Miyaji, D. W. Yoon and J. L. Sessler, *Chem. Commun.*, 2008, 24.

8 (*a*) L. P. Cao, M. Sekutor, P. Y. Zavalij, K. Mlinaric-Majerski, R. Glaser and L. Isaacs, *Angew. Chem., Int. Ed.*, 2014, **53**, 988; (*b*) S. Sonzini, A. Marcozzi, R. J. Gubeli, C. F. van der Walle, P. Ravn, A. Herrmann and O. A. Scherman, *Angew. Chem., Int. Ed.*, 2016, **55**, 14000.

9 (*a*) G. Yu, K. Jie and F. H. Huang, *Chem. Rev.*, 2015, **115**, 7240; (*b*) X. Chen, L. Hong, X. You, Y. Wang, G. Zou, W. Sua and Q. Zhang, *Chem. Commun.*, 2009, 1356; (*c*) L. Szente and J. Szemán, *Anal. Chem.*, 2013, **85**, 8024.

10 D.-C. Zhong and T.-B. Lu, *Chem. Commun.*, 2016, **52**, 10322.

11 (*a*) D. J. Cram, *Science*, 1988, **240**, 760; (*b*) J. M. Lehn, *Science*, 2002, **295**, 2400.

12 H. Zhou, Y. Zhao, G. Gao, S. Li, J. Lan and J. You, *J. Am. Chem. Soc.*, 2013, **135**, 14908.

13 (*a*) S. J. Barrow, S. Kasera, M. J. Rowland, J. del Barrio and O. A. Scherman, *Chem. Rev.*, 2015, **115**, 12320; (*b*) R.-L. Lin, G.-S. Fang, W.-Q. Sun and J.-X. Liu, *Sci. Rep.*, 2016, **6**, 39057; (*c*) J. Zhang, Y.-Y. Xi, Q. Li, Q. Tang, R. Wang, Y. Huang, Z.

Tao, S.-F. Xue, L. F. Lindoy and G. Wei, *Chem. – Asian J.*, 2016, **11**, 2250.

14 S. Huang, S. He, Y. Lu, F. Wei, X. Zeng and L. Zhaoab, *Chem. Commun.*, 2011, **47**, 2408.

15 K. Yazaki, N. Kishi, M. Akita and M. Yoshizawa, *Chem. Commun.*, 2013, **49**, 1630.

16 (*a*) H. Sohn, M. J. Sailor, D. Magde and W. C. Trogler, *J. Am. Chem. Soc.*, 2003, **125**, 3821; (*b*) J. I. Steinfeld and J. Wormhoudt, *Annu. Rev. Phys. Chem.*, 1998, **49**, 203.

17 (*a*) H. Sohn, R. M. Calhoun, M. J. Sailor and W. C. Trogler, *Angew. Chem., Int. Ed.*, 2001, **40**, 2104; (*b*) M. E. Germain and M. J. Knapp, *J. Am. Chem. Soc.*, 2008, **130**, 5422.

18 V. Béreau, C. Duhayon and J.-P. Sutter, *Chem. Commun.*, 2014, **50**, 12061.

19 H.-T. Feng and Y.-S. Zheng, *Chem. – Eur. J.*, 2014, **20**, 195.

20 (*a*) V. Bhalla, A. Gupta and M. Kumar, *Org. Lett.*, 2012, **14**, 3112; (*b*) P. B. Pati and S. S. Zade, *Tetrahedron Lett.*, 2014, **55**, 5290; (*c*) A. Chowdhury and P. S. Mukherjee, *J. Org. Chem.*, 2015, **80**, 4064; (*d*) Y. Xu, B. Li, W. Li, J. Zhao, S. Sun and Y. Pang, *Chem. Commun.*, 2013, **49**, 4764–4766; (*e*) P. C. A. Swamy and P. Thilagar, *Chem. – Eur. J.*, 2015, **21**, 8874.

21 (*a*) Y. Erande, S. Chemate, A. More and N. Sekar, *RSC Adv.*, 2015, **5**, 89482; (*b*) Y. Peng, A.-J. Zhang, M. Dong and Y.-W. Wang, *Chem. Commun.*, 2011, **47**, 4505; (*c*) G. Sivaraman, B. Vidya and D. Chellappa, *RSC Adv.*, 2014, **4**, 30828; (*d*) B. Gogoi and N. S. Sarma, *ACS Appl. Mater. Interfaces*, 2015, **7**, 11195; (*e*) R. Mitra and A. Saha, *ACS Sustainable Chem. Eng.*, 2017, **5**, 604.

22 (*a*) M. Hardouin–Lerouge, P. Hudhomme and M. Sallé, *Chem. Soc. Rev.*, 2011, **40**, 30; (*b*) D. Seebach and J. Gardiner, *Acc. Chem. Res.*, 2008, **41**, 1366; (*c*) G. Guichard and I. Huc, *Chem. Commun.*, 2011, **47**, 5933.

23 (*a*) T. W. Myers, T. J. Sherbow, J. C. Fettinger and L. A. Berben, *Dalton Trans.*, 2016, **45**, 5989; (*b*) J. J. Kiernicki, M. G. Ferrier, J. S. L. Pacheco, H. S. L. Pierre, B. W. Stein, M. Zeller, S. A. Kozimor and S. C. Bart, *J. Am. Chem. Soc.*, 2016, **138**, 13941.

24 A. Kalita, S. Hussain, A. H. Malik, N. V. V. Subbarao and P. K. Iyer, *J. Mater. Chem. C*, 2015, **3**, 10767.

25 (*a*) M. A. Zwijnenburg, E. Berardo, W. J. Peveler and K. E. Jelfs, *J. Phys. Chem. B*, 2016, **120**, 5063; (*b*) H.-T. Feng and Y.-S. Zheng, *Chem. – Eur. J.*, 2014, **20**, 195.

26 (*a*) M. Wang, G. Zhang, D. Zhang, D. Zhu and B. Z. Tang, *J. Mater. Chem.*, 2010, **20**, 1858; (*b*) Y. Li, F. Li, H. Zhang, Z. Xie, W. Xie, X. Xu, B. Li, F. Shen, L. Ye, M. Hanif, D. Ma and Y. Ma, *Chem. Commun.*, 2007, 231; (*c*) P. S. Hariharan, D. Moon and S. P. Anthony, *J. Mater. Chem. C*, 2015, **3**, 8381.

27 (*a*) A. Kundu, P. S. Hariharan, K. Prabakaran, D. Moon and S. P. Anthony, *Cryst. Growth Des.*, 2016, **16**, 3400; (*b*) S. P. Anthony, *Chem. – Asian J.*, 2012, **7**, 374; (*c*) A. Maity, F. Ali, H. Agarwalla, B. Anothumakkool and A. Das, *Chem. Commun.*, 2015, **51**, 2130.